Bivariate chain length and long chain branching distribution for copolymerization of olefins and polyolefin chains containing terminal double-bonds

*João B. P. Soares**

Department of Chemical Engineering, University of Waterloo,
Waterloo, Ontario, Canada N2L 3G1

Archie E. Hamielec

McMaster Institute for Polymer Production Technology,
Department of Chemical Engineering, McMaster University, Hamilton, Ontario,
Canada L8S 4L7

(Received: October 18, 1995; revised manuscript of November 21, 1995)

SUMMARY:
Polyolefins containing long chain branches can be synthesized using certain metallocene catalysts such as Dow Chemical's constrained geometry catalyst. These polyolefins combine the excellent mechanical properties of polymers with narrow molecular weight distribution with the easy processability of polymers containing long chain branches. A mathematical model for the chain length distribution for these novel polyolefins was derived from basic principles and an analytical solution for the chain length distributions of the populations containing different number of long chain branches per polymer molecule was obtained. The analytical solution agrees with the direct solution of the population balances and with a Monte-Carlo simulation model. It is also shown that this solution applies for copolymers using pseudo-kinetic rate constants and Stockmayer's bivariate distribution.

Introduction and literature review

Historical perspective

Prior to the publications by Lai et al.[1,2] and Swogger and Kao[3], there was no unambiguous experimental evidence in the literature that ionic catalyst systems such as Phillips chromium oxide, Ziegler-Natta, and metallocene catalyst systems, could be used to synthesize homopolyethylene or ethylene-α-olefin copolymers with long chain branches (LCB).

Lai et al.[1] synthesized these branched polyolefins, named by them as substantially linear polyolefins, using a particular type of metallocene catalyst (constrained geometry catalyst: CG-catalyst). Substantially linear polyolefins have a degree of long chain branching in the range of 0.01 to 3 LCB per 1000 carbon atoms. The polymerization is done in a continuous stirred-tank reactor (CSTR) operating at steady-state conditions and at high temperatures. An aliphatic solvent is used in the reactor and all of the polymer chains are in solution. In the example provided in their patent, the homopolyethylene synthesized under the recommended polymerization conditions had a long chain branching frequency of 0.34 LCB per 1000 carbon

 CCC 1022-1344/96/$05.00

atoms, as measured by carbon-13 nuclear magnetic resonance (^{13}C NMR) using the methodology proposed by Randall[4].

Swogger and Kao[3] presented further evidence for LCB formation using the synthesis conditions recommended by Lai et al.[1] Four homopolyethylenes were synthesized with a CG-catalyst in a CSTR under different operation conditions. These polyethylenes had long chain branching frequencies of 0.2, 0.44, 0.53, and 0.66 LCB per polymer molecule as measured by ^{13}C NMR and gel permeation chromatography (GPC). The authors presented a mathematical model for a CSTR which apparently predicted, with good accuracy, long chain branching frequencies, density of ethylene-1-octene copolymers, melt index, and finally I_{10}/I_2 ratios (I_{10}/I_2 is the melt index ratio using 10 kg and 2.16 kg weights). Unfortunately very little detail was given about the mathematical model.

Lai et al.[1] also presented some remarkable data on the effect of polydispersity on I_{10}/I_2 for polyolefins synthesized using classical heterogeneous titanium-based Ziegler-Natta catalysts and produced with CG-catalysts. It is generally accepted that classical Ziegler-Natta catalysts have multiple active center types and consequently produce polyolefins with broad molecular weight distributions[5] (MWD). Shear thinning, as expected, increases with increase in the breadth of MWD for polyolefins produced with Ziegler-Natta catalysts. On the other hand, polyolefins synthesized with CG-catalysts have narrow MWD, with polydispersity near the theoretical value of two for single-site type catalysts[6]. However, the I_{10}/I_2 ratio could be increased, at essentially constant polydispersity, by increasing the long chain branching frequency. In fact, these authors have shown how to synthesize polyolefins with narrow MWD and sufficient degree of long chain branching that combine the excellent mechanical properties of narrow MWD polyolefins (impact properties, tear resistance, environmental stress cracking resistance, tensile properties, etc.) with the good shear thinning of broad MWD linear polyolefins[7].

Sugawara[8] synthesized two ethylene-α-olefin copolymers (with densities of 0.906 and 0.912 g/cm^3) using the recommended procedure of Lai et al.[2] Sugawara constructed a calibration curve for a CSTR using data available in the patent application by Lai et al. and then used this calibration curve to find CSTR operation conditions to produce a polymer with very low level of long chain branching (called polymer A) and a polymer with a moderate level of long chain branching (called polymer B). He then compared polymers A and B with a conventional linear low-density polyethylene (LLDPE) sample and with a high-pressure low-density polyethylene (HP-LDPE) sample in terms of impact strength, processability, blown film processability, stability, and MD/TD balance of tear strength. Polymers A and B were superior in impact strength. Polymer B was superior to LLDPE but inferior to HP-LDPE in processability. Polymer B was significantly inferior to HP-LDPE in bubble stability. This superiority of HP-LDPE over polymer B was very likely due to the much higher levels of long chain branching in HP-LDPE polymers. Polymers A and B were inferior to both LLDPE and HP-LDPE in MD but superior to HP-LDPE in TD. Sugawara provided an interesting summary of property balances and the position of metallocene copolymers of ethylene-α-olefins in the balance of strength versus processability and moldability.

It seems that the target for metallocene polymers is to keep the MWD narrow but raise the level of long chain branching to further improve processability.

Long chain branch formation mechanisms

The most likely LCB formation mechanism with metallocene catalyst systems is terminal branching, a mechanism which has been known in the free-radical polymerization literature for many years[9]. In free-radical polymerization, macromonomers (a long chain molecule with a reactive carbon-carbon double-bond at its end) are generated via termination by disproportionation and via chain transfer to monomer. With metallocene catalyst systems, the facile β-hydride elimination reaction appears to be responsible for in-situ macromonomer formation with terminal vinyl unsaturation. Other reaction types, such as β-methyl elimination give the desired terminal vinyl group[10]. This can actually be the most important transfer mechanism in propylene polymerization when $(Me_5Cp)_2Ti$, $(Me_5Cp)_2Zr$, and $(Me_5Cp)_2Hf$ complexes (Me: CH_3, Cp: cyclopentadienyl) are used[7]. Therefore, these catalytic systems have the potential of producing poly(propylene) with long chain branches. To our best knowledge this possibility has not been explored to date. These and other chain transfer mechanisms are summarized in Tab. 1.

It is generally accepted that the most effective macromonomer for addition to the active center with the generation of a long trifunctional branch is the one with terminal vinyl unsaturation, probably due to steric effects.

Tab. 1. Source of unsaturation and mechanism of formation of dead polymer with terminal double-bond (macromonomers)[19]

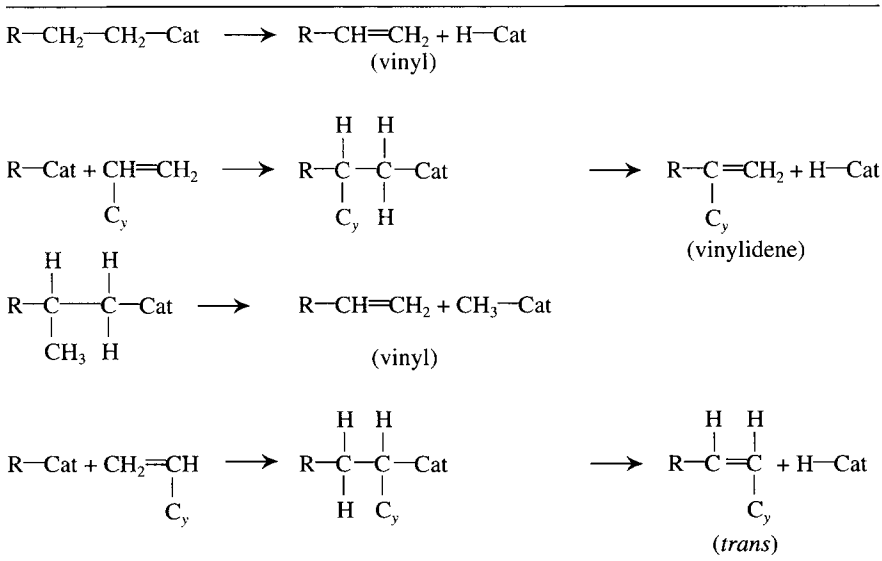

R: polymer chain; Cat: catalytic site; C_y: short chain branch containing y carbon atoms

Metallocene catalyst/cocatalyst types suitable for synthesis of polyolefins with long chain branches

The most suitable catalyst types appear to be those with an "open" metal active center, such as the Dow Chemical CG-catalysts. The active center of CG-catalysts is based on group IV transition metals (e.g. titanium) that are covalently bonded to a monocyclopentadienyl ring and bridged with a heteroatom, forming a constrained cyclic structure with the titanium center[1,2]. The bond angle between the monocyclopentadienyl ring, the titanium atom center, and the heteroatom is less than[11] 115°. Strong Lewis acid systems are used to activate the catalyst to a highly effective cationic form. This geometry allows the titanium center to be more "open" to the addition of monomer and higher α-olefins, but also for the addition of vinyl-terminated polymer molecules (macromonomers or dead polymer chains with terminal vinyl unsaturation). A second and very important requirement for the efficient production of polyolefins containing LCB's by these catalytic systems is that a high level of dead polymer chains with terminal vinyl unsaturation be produced continuously during the polymerization.

A suitable cocatalyst specified by Lai et al.[1] is tris(pentafluorophenyl)borane. There is no evidence in the literature that methylaluminoxane (MAO) cocatalysts are suitable for the synthesis of polyolefins containing LCB's.

Solvent types

Although there is not a great deal of evidence in the literature concerning optimal solvents for LCB formation, it appears that paraffinic solvents are preferable to aromatics. Lai et al.[1] recommend the use of aliphatic solvents for LCB synthesis. This choice was also supported by Brant et al.[12] for the catalytic system bis(cyclopentadienyl)zirconium dimethyl/perfluorotriphenylboron.

Polymerization processes which are suitable for LCB synthesis

Slurry polymerization

In slurry polymerization with soluble metallocene systems, the polymer molecules are insoluble in the solvent (also called the diluent). When polymer chains precipitate from solution, there is the possibility of two-phase polymerization, one occurring in the solvent phase and the other occurring in the polymer phase. Active centers and monomers may partition between these two phases, giving rise to different polymerization rates and to the formation of polymer chains with different MWD's in each of the two phases. In batch and semi-batch operation, phase volume ratios would change with time, giving overall polymerization rates and MWD's which would also change with time. However, the slurry polymerization of ethylene with bis(cyclopentadienyl)zirconium dichloride/MAO in toluene in a semi-batch reactor has a constant rate of polymerization and the polyethylene produced has polydispersity of two, suggesting that the active centers do not partition between the

two phases[13]. Although no conclusive evidence has been presented in the literature, it is generally accepted that the active sites remain in the solvent phase during the polymerization.

With supported metallocenes, which are insoluble in the solvent, active centers are encapsulated by polymer and the polymerization occurs almost exclusively in the polymer phase[14]. LCB formation should depend on the mobility of the macromonomers in the monomer/solvent swollen polymer particles. Self-diffusion coefficients of macromonomers depend on molecular weight and one therefore might expect that the rate of addition of a macromonomer to the active center is diffusion-controlled with preferential formation of shorter LCB's. On the other hand, the steric barrier for addition of a macromonomer also increases with size of reactant, retarding the addition of the longer macromonomers and, as a result, diffusion resistances may not be as important for larger macromolecules as one might expect (the controlling step may be overcoming the steric barrier at the metal center).

Gas-phase polymerization

In gas-phase reactors metallocene catalysts have to be supported prior to the polymerization[15]. With these processes, active centers are encapsulated in polymer and the limiting factor on LCB formation may be low levels of swelling of polymer particles by monomer and low self-diffusion coefficients of highly entangled polymer chains.

Solution polymerization

In solution processes, active centers and polymer chains are soluble in the solvent. These processes are generally carried out at temperatures above the melting temperatures of the polymer chains[1].

Solution processes are preferred to LCB synthesis for several reasons. Macromonomers with terminal vinyl unsaturation are formed at higher rates at elevated temperatures. These dissolved polymer chains are mobile and have relatively large diffusion coefficients. Most importantly, at these higher temperatures the steric barrier for the addition of a macromonomer to the active center is relatively less important than at lower temperatures.

A potential negative effect of these elevated temperatures is the reduced lifetime of the catalyst active centers. Short residence times can be used with a CSTR to overcome this problem. Shorter reactor residence times would also make product grade transitions more efficient.

Reactor operation conditions suitable for long chain branching synthesis

Batch operation

For batch operation, all of the ingredients (catalyst, cocatalyst, solvent, monomers, and chain transfer agents) are added to the reactor at time zero. Polymer con-

centration increases continuously with time until all of the monomers have been consumed. High polymer concentrations are reached only near the end of the polymerization, requiring long polymerization times to produce a significant amount of macromonomer and long chain branches. Unfortunately, particularly with solution polymerization at elevated temperatures, severe catalyst deactivation may take place during the polymerization and therefore long residence times would not be practical. To achieve desired LCB levels, higher polymer concentrations in solvent would likely be necessary, giving excessively high viscosities, problems with stirring, and increasing heat and mass transfer resistances.

Semi-batch operation

For semi-batch operation, all the ingredients, except for ethylene, are added to the reactor at time zero. The polymerization is done at constant temperature and pressure, with ethylene being fed on demand to maintain constant pressure. Semi-batch operation of the polymerization reactor has the same drawbacks as the batch operation. Additionally, the ethylene concentration in the solvent is essentially time-independent. For the same reactor pressure, the ratio of polymer to monomer concentration would be lower for semi-batch operation than for batch-operation, which is less favourable for LCB formation.

Continuous operation

For continuous operation at steady-state, all of the ingredients are fed into the reactor continuously. The polymer product, unreacted monomers and comonomers, and catalytic species leave the reactor continuously, and the temperature and concentrations of all species in the reactor are time-independent.

For continuous operation at steady-state, the residence-time distribution plays a very significant role in LCB generation. To illustrate this, we will consider the two extremes of a plug flow tubular reactor (PFTR) with a narrow residence time distribution and of a CSTR with a very broad residence time distribution. With the PFTR, the polymer concentration increases while the monomer concentration decreases as one moves along the reactor (similar to a batch reactor in time). High polymer concentrations are obtained near the exit of the PFTR, while much of the polymerizing mass in the reactor is at low polymer concentrations. With the CSTR, the entire reacting mass is at the same high polymer and low monomer concentration. The rates of LCB formation are clearly higher at higher polymer concentrations and rates of monomer consumption are clearly lower at lower monomer concentrations, giving high levels of long chain branching per mass of polymer. It should also be pointed out that with the CSTR, the concentration of ethylene in the polymerizing mass and exit stream is usually significantly lower than the equilibrium solubility at the operating temperature and pressure of the reactor. It is perfectly clear, therefore, that the optimal reactor type and operation conditions for maximum LCB formation is the steady-state operation of a continuous stirred tank reactor.

Model development

Kinetics of polymerization

The kinetics of polymerization considered for the present mathematical model includes steps of propagation, long chain branch formation via reaction with dead polymer chains containing terminal vinyl double-bonds, transfer to chain transfer agent (generating dead polymer chains with saturated chain-ends), and β-hydride elimination (generating dead polymer chains with terminal vinyl unsaturation). The initiation step is considered to be very fast and is not directly accounted for in the kinetics of polymerization.

$$
\begin{array}{lcll}
P_{r,i} + M & \rightarrow & P_{r+1,i} & k_p \\
P_{r,i} + D^{=}_{q,j} & \rightarrow & P_{r+q,i+j+1} & k_{pLCB} \\
P_{r,i} + CTA & \rightarrow & D_{r,i} + P_{1,0} & k_{CTA} \\
P_{r,i} & \rightarrow & D^{=}_{r,i} + P_{1,0} & k_\beta
\end{array}
$$

where,

$P_{r,i}$	living polymer of chain length r containing i long chain branches
$D^{=}_{q,j}$	dead polymer of chain length q containing j long chain branches and terminal vinyl unsaturation
$D_{q,j}$	dead polymer of chain length q containing j long chain branches and a saturated chain-end
M	monomer
CTA	chain transfer agent
k_p	propagation rate constant for monomer, in L/(mol · s)
k_{pLCB}	propagation rate constant for dead polymer with terminal double-bond, in L/(mol · s)
k_{CTA}	rate constant for transfer to chain transfer agent, in L/(mol · s)
k_β	rate constant for β-hydride elimination, in 1/s

Dead polymer chains having terminal vinyl unsaturation, $D^{=}_{q,j}$ can coordinate to the catalytic active site and insert in the growing chain, forming a trifunctional LCB. Dead polymer chains with saturated chain ends, $D_{q,j}$ can not polymerize again. Observe that, by examining the mechanism of chain formation, one can conclude that the instantaneous molecular weight distributions of live polymer, dead polymer with chain-end unsaturation, and dead polymer with saturated chain-ends will be the same. However, the relative amount of dead polymer with and without terminal vinyl unsaturation is proportional to the rates of β-hydride elimination (producing dead polymer chains with terminal vinyl unsaturation), and transfer to chain transfer agent (commonly to hydrogen, producing dead polymer chains with saturated chain-ends).

The equations derived below can be easily modified if other types of transfer reactions need to be considered.

Population balances

The concentration of dead polymer chains in the reactor is given by

$$\frac{dD^{=}_{r,i}}{dt} = k_\beta P_{r,i} - (k_{pLCB} Y_0 + s) D^{=}_{r,i} \tag{1}$$

$$\frac{dD_{r,i}}{dt} = k_{CTA}[CTA] P_{r,i} - s D_{r,i} \tag{2}$$

where s is the reciprocal of the mean residence time in the reactor and Y_0 is the zeroth moment of living polymer chains,

$$Y_0 = \sum_{r=1}^{\infty} \sum_{i=0}^{\infty} P_{r,i} \tag{3}$$

Similar equations can be derived for the living polymer chains:

$$\frac{dP_{1,0}}{dt} = K_T Y_0 - P_{1,0}(k_p M + k_{pLCB} Q_0^{=}) + s(Y_0 - P_{1,0}) \tag{4}$$

$$\begin{aligned} \frac{dP_{r,i}}{dt} =& k_p M (P_{r-1,i} - P_{r,i}) \\ &+ k_{pLCB} \sum_{s=1}^{r-1} \sum_{j=0}^{i-1} P_{r-s,j} D^{=}_{s,i-1-j} - (K_T + k_{pLCB} Q_0^{=} + s) P_{r,i} \end{aligned} \tag{5}$$

where $Q_0^{=}$, the zeroth moment of dead polymer chains containing a terminal double-bond, is given by:

$$Q_0^{=} = \sum_{r=1}^{\infty} \sum_{i=0}^{\infty} D^{=}_{r,i} \tag{6}$$

and

$$K_T = k_\beta + k_{CTA}[CTA] \tag{7}$$

Assuming steady-state operation in a CSTR, the populations of dead and living polymer are easily obtained from Eqs. (1), (2), and (5):

$$D^{=}_{r,i} = \frac{k_\beta}{k_{pLCB} Y_0 + s} P_{r,i} \tag{8}$$

$$D_{r,i} = \frac{k_{CTA}[CTA]}{s} P_{r,i} \tag{9}$$

$$P_{r,i} = \frac{k_p M}{\gamma} P_{r-1,i} + \frac{k_{pLCB}}{\gamma} \sum_{s=1}^{r-1} \sum_{j=0}^{i-1} P_{r-s,j} D^{=}_{s,i-1-j} \tag{10}$$

Substituting Eq. (8) in (10), the population of living polymer becomes:

$$P_{r,i} = A P_{r-1,i} + B \sum_{s=1}^{r-1} \sum_{j=0}^{i-1} P_{r-s,j} P_{s,i-1-j} \tag{11}$$

where,

$$A = \frac{k_p M}{\gamma} \tag{12}$$

$$B = \frac{k_{pLCB} k_\beta}{\gamma(k_{pLCB} Y_0 + s)} \tag{13}$$

$$\gamma = k_p M + K_T + k_{pLCB} Q_0^{=} + s \tag{14}$$

At steady-state, $P_{1,0}$ is easily calculated from Eq. (4):

$$P_{1,0} = \frac{(K_T + s) Y_0}{k_p M + k_{pLCB} Q_0^{=} + s} \tag{15}$$

and $Q_0^{=}$ can be calculated from Eq. (1):

$$\frac{dQ_0^{=}}{dt} = \frac{d\left(\sum_{r=1}^{\infty}\sum_{i=0}^{\infty} D_{r,i}^{=}\right)}{dt} = k_\beta Y_0 - (k_{pLCB} Y_0 + s) Q_0^{=} = 0 \tag{16}$$

and therefore,

$$Q_0^{=} = \frac{k_\beta Y_0}{k_{pLCB} Y_0 + s} \tag{17}$$

The numerical solution of Eqs. (8), (9), and (11) will give the exact results for the chain length and LCB distribution of live and dead polymer. However, the solution of these equations is very time consuming. The living polymer chains have to be calculated sequentially, starting with linear polymer chains of chain length one, up to polymer chains with chain length r and n LCB. Observe that the computation of the summation term of Eq. (11) becomes very time consuming as the chain length increases.

Notice that the MWD's of living and dead polymer chains are the same, since the population balances for dead polymer only differ by a constant value from the population balance for living polymer, as shown in Eq. (8) and (9).

Moment equations and chain length averages

Chain length averages for the several chain populations as a function of the number of LCB's per chain can be calculated by the method of moments. Moment equations for the living polymer are dfined as follows

$$\bar{r}_{n,i} = \frac{Y_{1,i}}{Y_{0,i}} = \frac{\sum_{r=1}^{\infty} r P_{r,i}}{\sum_{r=1}^{\infty} P_{r,i}} \tag{18}$$

$$\bar{r}_{w,i} = \frac{Y_{2,i}}{Y_{1,i}} = \frac{\sum_{r=1}^{\infty} r^2 P_{r,i}}{\sum_{r=1}^{\infty} r P_{r,i}} \tag{19}$$

$$\bar{r}_{z,i} = \frac{Y_{3,i}}{Y_{2,i}} = \frac{\sum_{r=1}^{\infty} r^3 P_{r,i}}{\sum_{r=1}^{\infty} r^2 P_{r,i}} \tag{20}$$

$$\text{pdi}_i = \frac{\bar{r}_{w,i}}{\bar{r}_{n,i}} \tag{21}$$

where,

$\bar{r}_{n,i}$ number-average chain length for population with i LCB/chain
$\bar{r}_{w,i}$ weight-average chain length for population with i LCB/chain
$\bar{r}_{z,i}$ z-average chain length for population with i LCB/chain
pdi_i polydispersity index for population with i LCB/chain
$Y_{j,i}$ j^{th} moment of the distribution for population with i LCB/chain

Observe that chain length averages for dead polymer (with or without terminal vinyl unsaturation) are the same as for living polymer, as can easily be seen from Eqs. (8) and (9). Therefore, only expressions for living polymer will be presented.

Equations for the moments of the distributions are derived in Appendix A. It can be shown that the chain length averages of the different populations are related by the simple expressions

$$\bar{r}_{n,0} = \frac{k_{pLCB} M}{\phi} \tag{22}$$

$$\bar{r}_{w,0} = 2\frac{k_{pLCB} M}{\phi} \tag{23}$$

$$\bar{r}_{z,0} = 3\frac{k_{pLCB} M}{\phi} \tag{24}$$

$$\text{pdi}_0 = 2 \tag{25}$$

$$\bar{r}_{n,i} = (1 + 2i)\bar{r}_{n,0} \tag{26}$$

$$\bar{r}_{w,i} = (1 + i)\bar{r}_{w,0} \tag{27}$$

$$\bar{r}_{z,i} = (1 + 2i/3)\bar{r}_{z,0} \tag{28}$$

$$\text{pdi}_i = \left(\frac{1+i}{1+2i}\right)\text{pdi}_0 \tag{29}$$

where

$$\phi = K_T + k_{pLCB}Q_0^{=} + s \tag{30}$$

Bivariate distributions of chain length and long chain branching

For linear chains, Eq. (11) reduces to Flory's most probable distribution:

$$P_{r,0} = A^{r-1}P_{1,0} \tag{31}$$

Similarly, for chains that have only one LCB:

$$P_{r,1} = AP_{r-1,1} + B\sum_{s=1}^{r-1} P_{r-s,0}P_{s,0} \tag{32}$$

Eq. (32) can be further simplified by noticing that $P_{r-s,0}$ and $P_{s,0}$ can be calculated by Eq. (31):

$$P_{r-s,0} = A^{r-s-1}P_{1,0} \tag{33}$$

and

$$P_{s,0} = A^{s-1}P_{1,0} \tag{34}$$

Substituting Eqs. (33) and (34) in Eq. (32) and expanding the summation term, one obtains:

$$P_{r,1} = AP_{r-1,1} + A^{r-2}B(r-1)P_{1,0}^2 \tag{35}$$

Eq. (35) can then be used to calculate $P_{r-1,1}$:

$$P_{r-1,1} = AP_{r-2,1} + A^{r-3}B(r-2)P_{1,0}^2 \tag{36}$$

which, upon substitution in Eq. (35) leads to:

$$P_{r,1} = A^2P_{r-2,1} + A^{r-2}BP_{1,0}^2[(r-1)+(r-2)] \tag{37}$$

$P_{r-2,1}$ can also be calculated using Eq. (35) and the resulting equation substituted in Eq. (37). These steps are repeated until one obtains an expression for $P_{r,1}$ as a function of $P_{1,0}$:

$$P_{r,1} = \frac{1}{2}A^{r-2}BP_{1,0}^2r^2 \tag{38}$$

The same procedure can be used to obtain the chain length distribution of populations containing 2, 3, 4, ..., n LCB/chain. For polymer chains with 2 LCB (Appendix B), Eq. (11) becomes:

$$P_{r,2} = AP_{r-1,2} + B\sum_{s=1}^{r-1}(P_{r-s,0}P_{s,1} + P_{r-s,1}P_{s,0}) \tag{39}$$

Eq. (31) can be used to calculate $P_{r-s,0}$ and $P_{s,0}$ and Eq. (38) to calculate $P_{s,1}$ and $P_{r-s,1}$ By substitution into Eq. (39) and repetition of this procedure for $P_{r-1,2}$, $P_{r-2,2}$, $P_{r-3,2}$, ..., one obtains the final chain length distribution for chains with 2 LCB:

$$P_{r,2} = \frac{1}{12} A^{r-3} B^2 P_{1,0}^3 r^4 \tag{40}$$

It is shown in Appendix B that the distribution of chain length for populations containing n LCB/chain can be represented by the general expression:

$$P_{r,n} = \frac{1}{(n+1)\prod_{i=0}^{n-1}(n-i)^2} A^{r-1-n} B^n P_{1,0}^{n+1} r^{2n} \tag{41}$$

Notice that Eq. (41) can be substituted into Eqs. (8) and (9) to obtain the chain length distribution of dead polymer with and without terminal vinyl unsaturation, respectively.

Bivariate frequency distribution of chain length and long chain branching

In Eq. (41), $P_{r,n}$ is the concentration of polymer chains of chain length r that have n LCB's. Frequency distributions can be derived for each chain population containing n LCB's by normalizing Eq. (41).

For linear chains:

$$f(r,0) = \frac{A^{r-1} P_{1,0}}{\sum_{r=1}^{\infty} A^{r-1} P_{1,0}} = \frac{A^{r-1}}{\sum_{r=1}^{\infty} A^{r-1}} \tag{42}$$

For long chains, $A \to 1$, and Eq. (42) reduces to

$$f(r,0) = A^r(1-A) = \tau \exp(-r\tau) \tag{43}$$

where $\tau = 1 - A$.

Analogously, for the population of chains with one LCB/chain:

$$f(r,1) = \frac{(1/2)A^{r-2} B P_{1,0}^2 r^2}{\sum_{r=2}^{\infty}(1/2)A^{r-2} B P_{1,0}^2 r^2} \quad \frac{A^{r-2} r^2}{\sum_{r=2}^{\infty} A^{r-2} r^2} \tag{44}$$

For long chains Eq. (44) can be simplified to:

$$f(r,1) = \frac{1}{2} A^{r-4} r^2 (1-A)^3 \tag{45}$$

Repeating these steps for populations of polymer chains with increasing number of LCB/chain (Appendix C), one obtains the final frequency distribution of chain length for polymer chains with n LCB:

$$f(r,n) = \frac{1}{(2n)!} A^{r-1-3n} r^{2n} (1-A)^{2n+1} \tag{46}$$

or, equivalently,

$$f(r,n) = \frac{1}{(2n)!} r^{2n} \tau^{2n+1} \exp(-r\tau) \tag{47}$$

These distributions have the same chain length averages as predicted by the method of moments, Eqs. (22) to (29) (Appendix C).

Simulation results and discussion

Fig. 1 a and 1 b show the chain length distributions predicted with the derived analytical solution. Notice that the individual distributions are normalized with respect

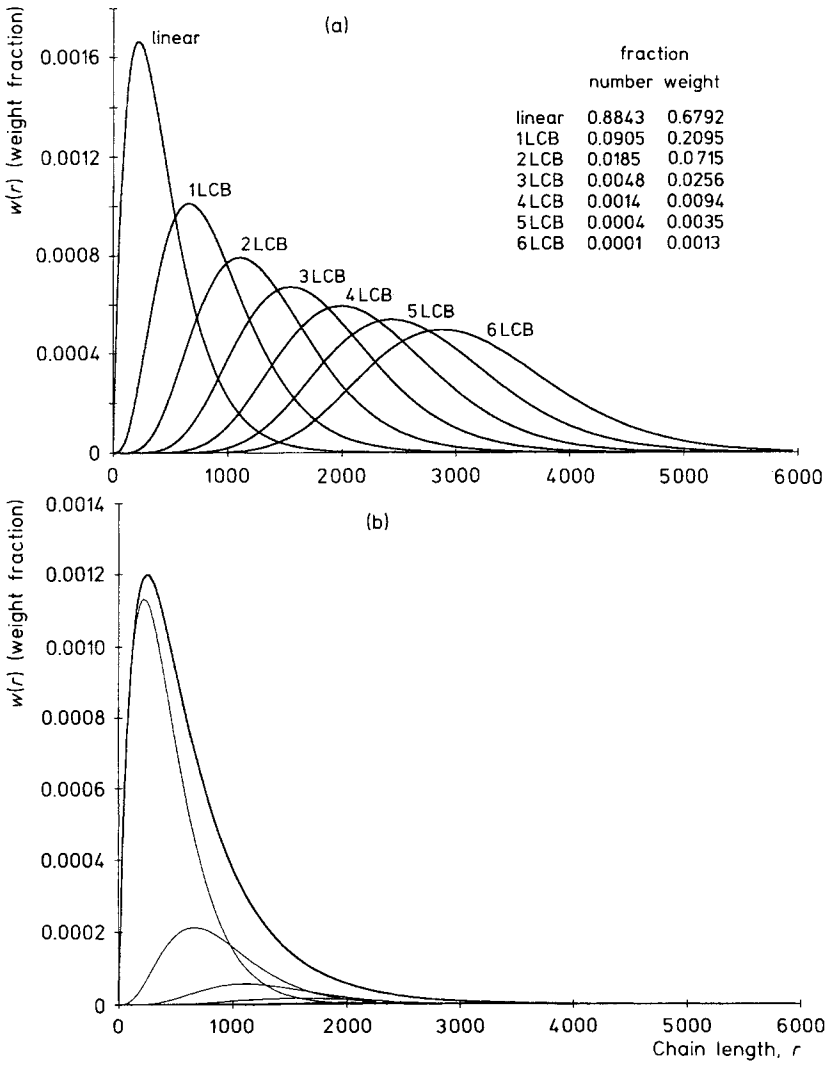

Fig. 1. Chain length distribution for polymer populations containing different number of LCB per chain: (a) weight chain length distributions normalized for each individual population, $\tau = 0.004507$; (b) weight chain length distribution normalized with respect to the total weight of the whole polymer, $\tau = 0.004507$, $B = 51.93875$. The global distribution (over all polymer populations) is indicated by the bold line and is apparently unimodal ($\bar{B}_N = 0.15$, $\bar{r}_n = 287$, pdi = 2.30). The table in the top right corner indicates number and weight fractions of each population

to the total weight of chains in the whole polymer in Fig. 1b. Under these polymerization conditions, the degree of long chain branching is 0.15, and the number-average chain length and polydispersity are 287 and 2.30, respectively. These average values were obtained by integrating the global chain length distribution shown in Fig. 1b. Fig. 1a and 1b reveal the absolute variance of each population. However, to assess whether the distribution breadth increases or decreases with branching level, one should compare coefficients of variation and then it is clear that distribution breadths decrease significantly with increase in long chain branching level.

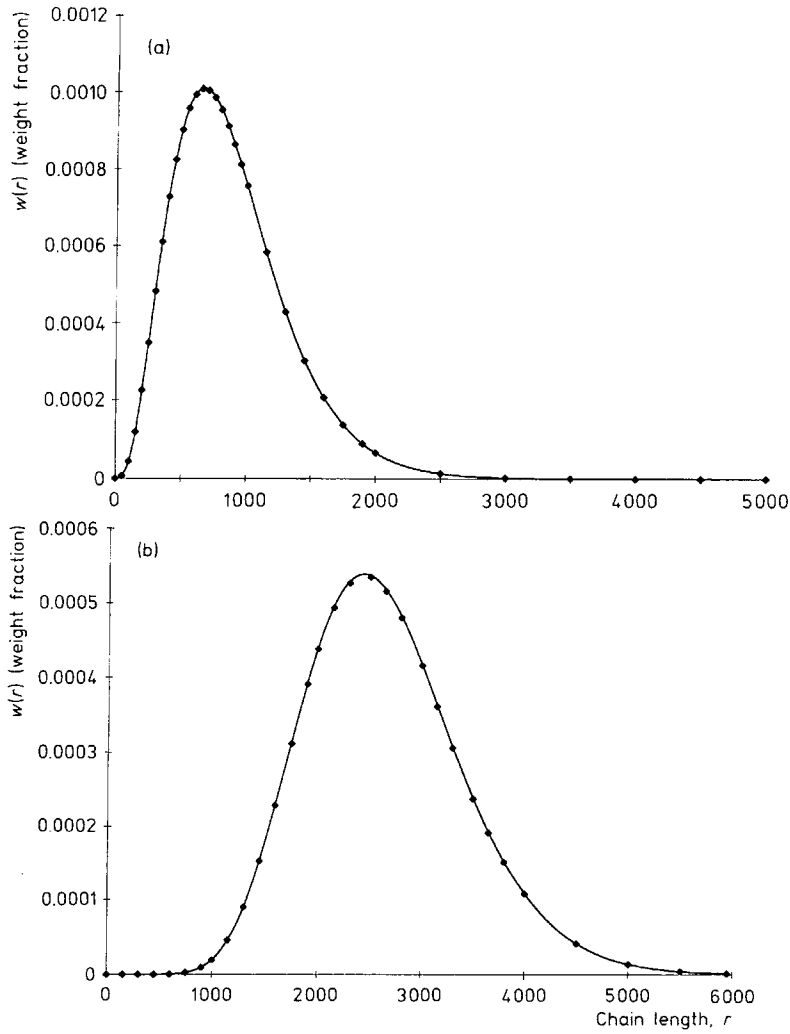

Fig. 2. Comparison of weight chain length distributions obtained by numerical solution of Eq. (11), and using the analytical solution, Eq. (41): (a) 1 LCB/polymer chain; (b) 5 LCB/polymer chain. ◆: Numerical solution; ——: analytical solution

To assess the validity of these results, the analytical solution was compared with the direct solution of the steady-state population balances and with a chain length distribution generated by a Monte-Carlo simulation model. Fig. 2a and 2b compare the analytical solution with the distribution obtained by solving the population balances given by Eq. (11). The agreement between the two solutions is excellent. This indicates that both the analytical and numerical solutions correctly represent the steady-state population balances defined by Eq. (11).

A Monte-Carlo model was developed to further validate the derived analytical solution. Fig. 3a to 3c compare the distributions predicted with the analytical solution and with the Monte-Carlo method. The agreement between the two solutions is again excellent. This is a good indication that the analytical solution is valid and the Monte-Carlo calculations have acceptable accuracy. It also indicates that this analytical solution can be used for polymerization processes that can be described by a simple model that accounts only for probabilities of polymerization and termination, as used in the Monte-Carlo model.

A population of 70×10^6 chains were generated by the Monte-Carlo simulation model. Notice that the Monte-Carlo simulation results become noisier for higher degrees of long chain branching because the number of polymer chains generated in the simulation decreases with increasing degree of long chain branching.

The Monte-Carlo model generates polymer chains sequentially using a probability of propagation, P_{pT}, and a probability of termination, P_t so that:

$$P_{pT} + P_t = 1 \tag{48}$$

If a chain propagates, it can either add a monomer with probability P_p or a macromonomer with probability P_{pLCB} so that:

$$P_p + P_{pLCB} = 1 \tag{49}$$

For long chain branch formation, a macromonomer is selected randomly from the already generated population of macromonomers.

Probabilities of propagation and termination can be obtained from polymerization kinetic data and reactor operation conditions by noticing that:

$$P_{pT} = \frac{k_p M + k_{pLCB} Q_0^{=}}{k_p M + k_{pLCB} Q_0^{=} + K_T} \tag{50}$$

$$P_{pLCB} = \frac{k_{pLCB} Q_0^{=}}{k_p M + k_{pLCB} Q_0^{=}} \tag{51}$$

The distribution generated for linear chains using the Monte-Carlo model follows Flory's most probable distribution, indicating that the method has acceptable accuracy. Fig. 4 presents the fluxogram for the Monte-Carlo model used in this study.

Molecular weight averages and degrees of long chain branching calculated by direct solution of the population balances, by the Monte-Carlo model, and with the proposed analytical solution are compared in Tab. 2.

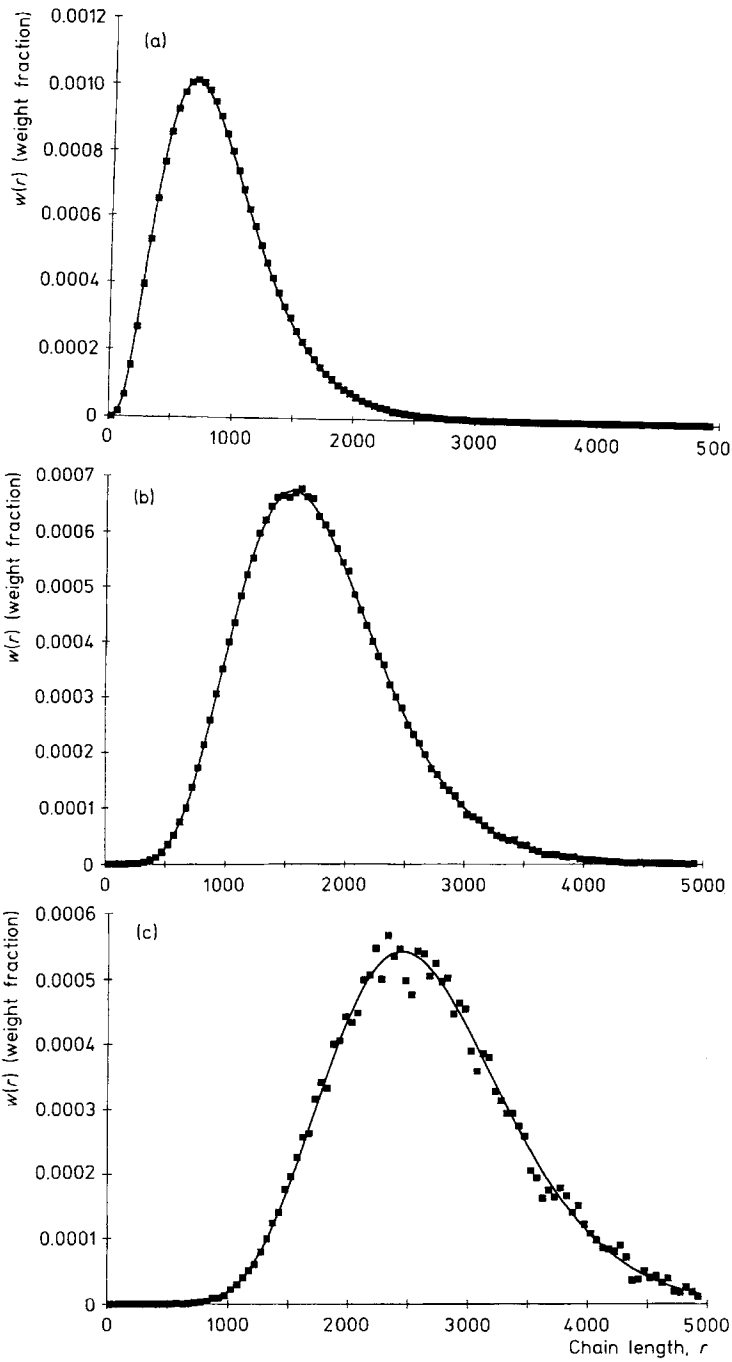

Fig. 3. Comparison of weight chain length distributions simulated with the Monte-Carlo model, and using the analytical solution, Eq. (47) (P_{pT} = 0.996018, P_{plCB} = 0.000521): (a) 1 LCB/polymer chain; (b) 3 LCB/polymer chain; (c) 5 LCB/ polymer chain. ■: Monte Carlo; ——: analytical

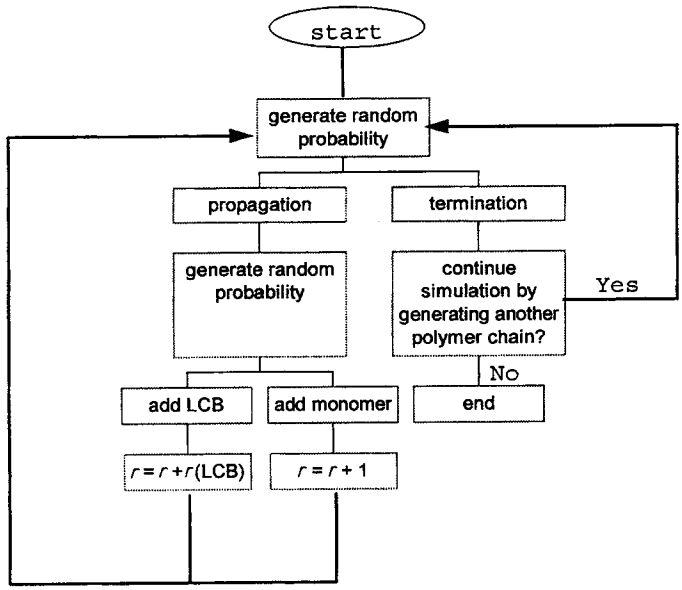

Fig. 4. Fluxogram for Monte-Carlo model

Tab. 2. Comparison of chain length averages and degree of long chain branching calculated by direct solution of population balances, Monte Charlo method, and analytical solution

	Direct solution, Eq. (11)	Monte-Carlo model, Fig. 4	Analytical solution, Eq. (41)
$\bar{r}_n$	289	289	288
$\bar{r}_w$	661	664	662
$\bar{r}_z$	1110	1117	1110
pdi	2.29	2.30	2.30
$\bar{B}_N$	0.15	0.15	0.15

Fig. 5 compares some case-studies for different rates of macromonomer addition. As expected, increasing the degree of long chain branching increases the high molecular weight tail of the distribution and consequently increases the polydispersity index. Average values for molecular weights and degrees of long chain branching for the simulations shown in Fig. 5 are presented in Tab. 3.

A similar result could be obtained for the effect of different residence-times in the reactor on chain length distribution. Increasing residence-time will increase the degree of long chain branching, since longer residence times in the reactor increase the concentration of polymer with terminal vinyl unsaturation and reduce the monomer concentration in the reactor. It is clear that different residence-time distributions and mean residence-times for the reactor will have a decisive influence on the

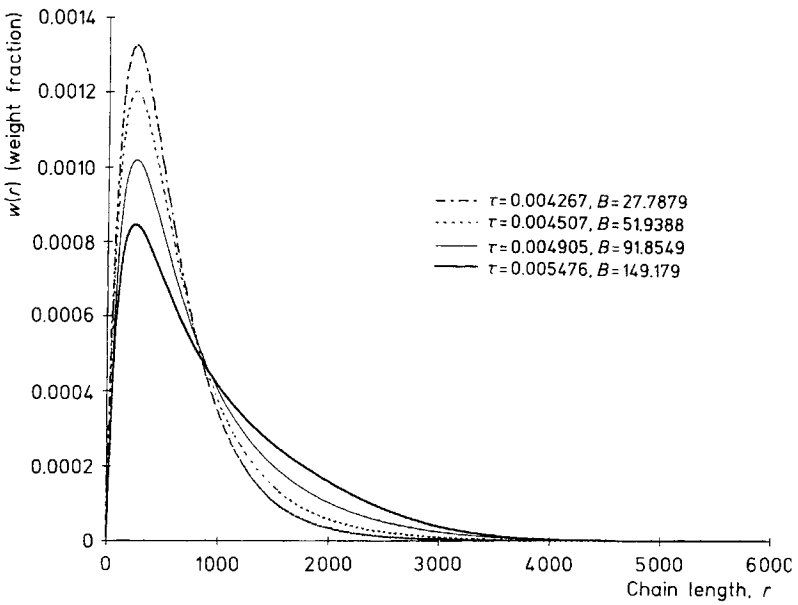

Fig. 5. Effect of varying macromonomer addition rate on weight chain length distribution. See average values for chain length and long chain branching in Tab. 3

Tab. 3. Chain length averages and degree of long branching as a function of k_{pLCB}

k_{pLCB} L/(mol·s)	$\bar{B}_N$	$\bar{r}_n$	$\bar{r}_w$	$\bar{r}_z$	pdi
30	0.075	268	580	928	2.16
60	0.150	288	662	1110	2.30
120	0.290	320	806	1378	2.51
240	0.500	363	952	1556	2.62

degree of long chain branching of the polymer product. This is an important factor for scale-up and design of the polymerization reactors.

As can be seen from Fig. 1 a, the chain length distributions become narrower and more symmetrical with increasing number of LCB per polymer chain. This can be easily seen from Eq. (29) for polydispersity index. In the limit, as the number of LCB's tends to infinity, the polydispersity index tends to 1, i.e., the polymer population has a monodisperse distribution of chain lengths. Fig. 6 shows this functional dependency.

The chain length distribution of the long chain branches can also be easily obtained from the proposed distribution. Since all long branches are formed by the reaction of living polymer and dead polymer with terminal vinyl unsaturation, the

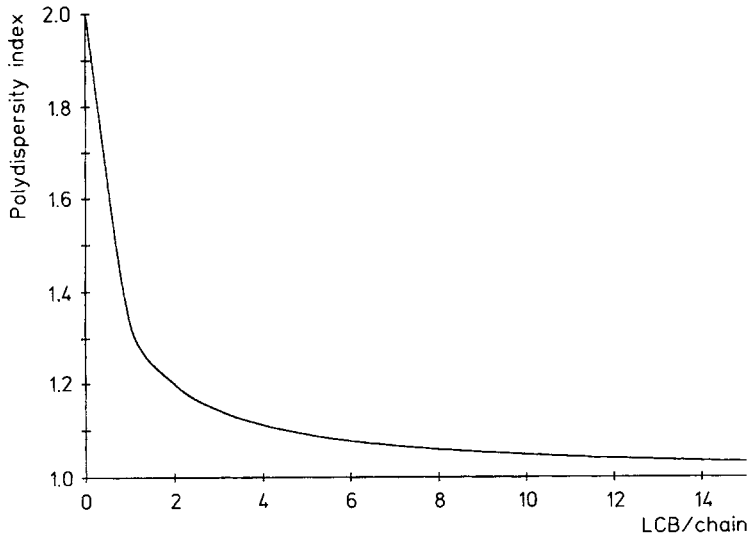

Fig. 6. Polydispersity index as a function of number of LCB per polymer molecule

same chain length distribution applies for the long chain branches. In this way, all linear branches follow Flory's most probable distribution (i.e., Eq. (47) with $n = 0$). Similarly, all long chain branches that contain k long chain branches follow Eq. (47) with $n = k$.

Although Eq. (47) was derived for the case of homopolymerization, it can be easily extended for copolymerization by defining pseudo-kinetic rate constants[9,16] as shown in Appendix D. For the case of binary copolymerization, the chemical composition of the linear chains can be directly obtained by Stockmayer's bivariate distribution[17]. Since the long chain branching mechanism will not alter the composition of the polymer chains, Stockmayer's distribution will also apply for the branched chains.

It is also evident that the proposed analytical solution can be used as instantaneous chain length distribution for non-steady-state operation of a CSTR or other reactor types. In this way, the cumulative chain length distribution can be obtained by tracking changes to the instantaneous distribution due to long chain branching in time for other reactor types and operation conditions[16,17].

Conclusions

The molecular weight distribution of polyolefins containing long chain branches formed by the mechanism of terminal branching can be described by a simple analytical mathematical expression. This analytical solution agrees very well with the distribution predicted by directly solving the population balances and with the distribution generated using a Monte-Carlo model.

This analytical solution can be used to obtain the cumulative chain length distribution of polyolefins produced in a CSTR operating at steady-state. It also predicts the instantaneous chain length distribution of polymer produced during non-steady-state operation of a CSTR or in other types of reactors.

It was shown that the distribution can be easily modified to account for copolymerization using Stockmayer's bivariate distribution and the pseudo-kinetic constant method.

Appendix A: Expression for chain length averages from the method of moments

Chain length averages can be obtained from the knowledge of the moments of the distribution of polymer chains, as given by Eqs. (18) to (20). Observe that chain length averages for linear and dead polymer (with and without terminal double-bond) are the same.

The m^{th} moment of the distribution of chain length of living polymer is defined as:

$$Y_{m,i} = \sum_{r=1}^{\infty} r^m P_{r,i} \tag{A.1}$$

Substituting Eqs. (4) and (5) in Eq. (A.1) for linear chains ($i = 0$),

$$Y_{0,0} = \frac{(K_T + s)Y_0 + K_T P_{1,0}}{\phi} \cong \frac{(K_T + s)Y_0}{\phi} \tag{A.2}$$

$$Y_{1,0} = \frac{(K_T + s)Y_0 + k_p M Y_{0,0} + K_T P_{1,0}}{\phi} \cong \frac{(K_T + s)Y_0 + k_p M Y_{0,0}}{\phi} \tag{A.3}$$

$$\begin{aligned} Y_{2,0} &= \frac{(K_T + s)Y_0 + k_p M(2Y_{1,0} + Y_{0,0}) + K_T P_{1,0}}{\phi} \\ &\cong \frac{(K_T + s)Y_0 + k_p M(2Y_{1,0} + Y_{0,0})}{\phi} \end{aligned} \tag{A.4}$$

where Y_0 and ϕ are defined by Eqs. (3) and (30), respectively. Therefore, chain length averages are calculated by the following equations:

$$\bar{r}_{n,0} = \frac{Y_{1,0}}{Y_{0,0}} = 1 + \frac{k_p M}{\phi} \cong \frac{k_p M}{\phi} \tag{A.5}$$

$$\bar{r}_{w,0} = \frac{Y_{2,0}}{Y_{1,0}} = 1 + 2\frac{k_p M}{\phi} \cong 2\frac{k_p M}{\phi} \tag{A.6}$$

$$\text{pdi}_0 = 2 \tag{A.7}$$

since $\frac{k_p M}{\phi} \gg 1$ for long chains.

Similarly, for chains containing only one LCB/chain,

$$Y_{0,1} = \frac{k_{pLCB} Y_{0,0} Q^{=}_{0,0}}{\phi} \tag{A.8}$$

$$Y_{1,1} = \frac{k_p M Y_{0,1} + k_{pLCB}(Q^{=}_{0,0} Y_{1,0} + Q^{=}_{1,0} Y_{0,0})}{\phi} \tag{A.9}$$

$$Y_{2,1} = \frac{k_p M(2Y_{1,1} + Y_{0,1}) + k_{pLCB}(Q^{=}_{0,0} Y_{2,0} + 2Q^{=}_{1,0} Y_{1,0} + Q^{=}_{2,0} Y_{0,0})}{\phi} \tag{A.10}$$

where the moments of the dead polymer chains having terminal vinyl-unsaturation are given by:

$$Q^{=}_{m,i} = \sum_{r=1}^{\infty} r^m D^{=}_{r,i} = \alpha Y_{m,i} \tag{A.11}$$

and

$$\alpha = \frac{k_\beta}{k_{pLCB} Y_0 + s} \tag{A.12}$$

Making the long chain assumption, one obtains the following expression for chain length averages:

$$\bar{r}_{n,1} = \frac{Y_{1,1}}{Y_{0,1}} = \frac{k_p M}{\phi} + 2\frac{Y_{1,0}}{Y_{0,0}} \equiv 3\bar{r}_{n,0} \tag{A.13}$$

$$\bar{r}_{w,1} = \frac{Y_{2,1}}{Y_{1,1}} = 5 + 2\bar{r}_{w,0} \equiv 2\bar{r}_{w,0} \tag{A.14}$$

$$\mathrm{pdi}_1 = \frac{4}{3} \tag{A.15}$$

The same calculations can be repeated for populations with 2, 3, ..., n LCB/chain, resulting on the general relationships presented in Eqs. (26) to (29). All derivation steps were verified with MAPLE V [18].

It is interesting to notice that, for low levels of long chain branching, the polydispersity index for the whole polymer (considering all populations) can be estimated by the simple expression:

$$\mathrm{pdi} = \frac{\bar{r}_w}{\bar{r}_n} + 2(1 + \bar{B}_N) \tag{A.16}$$

For the conditions shown in Tab. 3 and Fig. 5, Eq. (A.16) predicts values of 2.15, 2.30, 2.58, and 3.00 for pdi. As can be seen from Tab. 3, considerable deviations are only observed for $\bar{B}_N = 0.5$.

Appendix B: Derivation of bivariate distribution

For the population with two LCB/chain, Eq. (10) becomes:

$$P_{r,2} = AP_{r-1,2} + B\sum_{s=1}^{r-1}(P_{r-s,0}P_{s,1} + P_{r-s,1}P_{s,0}) \tag{B.1}$$

Using Eq. (31) to calculate $P_{r-s,0}$ and $P_{s,0}$ and Eq. (38) to calculate $P_{s,1}$ and $P_{r-s,1}$, Eq. (B.1) becomes:

$$P_{r,2} = AP_{r-1,2} + \frac{A^{r-3}B^2P_{1,0}^3}{2}\sum_{s=1}^{r-1}[(s-1)s + (r-s-1)(r-s)] \tag{B.2}$$

Therefore,

$$P_{r-1,2} = AP_{r-2,2} + \frac{A^{r-4}B^2P_{1,0}^3}{2}\sum_{s=1}^{r-2}[(s-1)s + (r-s-2)(r-s-1)] \tag{B.3}$$

Substituting (B.3) in (B.2),

$$\begin{aligned} P_{r,2} = A^2P_{r-2,2} + \frac{A^{r-3}B^2P_{1,0}^3}{2}\Bigg\{ &\sum_{s=1}^{r-1}[(s-1)s + (r-s-1)(r-s)] \\ &+ \sum_{s=1}^{r-2}[(s-1)s + (r-s-2)(r-s-1)]\Bigg\} \end{aligned} \tag{B.4}$$

Repeating this procedure until the first term on the right-hand side of Eq. (B.4) is $P_{3,2}$ (which can be set equal to zero), one obtains:

$$P_{r,2} = \frac{A^{r-3}B^2P_{1,0}^3}{2}\sum_{i=1}^{r-1}\sum_{s=1}^{r-i}[(s-1)s + (r-s-i)(r-s+i)] \tag{B.5}$$

For long chains, the summation term of Eq. (B.5) is simply $r^4/6$ and it can be simplified to:

$$P_{r,2} = \frac{1}{12}A^{r-3}B^2P_{1,0}^2r^4 \tag{B.6}$$

This procedure can be repeated for populations with 3, 4, ..., n LCB/chain to obtain the final distribution shown in Eq. (41). All derivations were verified using MAPLE V [18].

Appendix C: Derivation of bivariate frequency distribution

For the population with only one LCB/chain, Eq. (41) becomes:

$$P_{r,1} = \frac{1}{2}A^{r-2}BP_{1,0}^2r^2 \tag{C.1}$$

Eq. (C.1) is easily normalized to give the frequency distribution:

$$f(r,1) = \frac{(1/2)A^{r-2}BP_{1,0}^2 r^2}{\sum_{r=2}^{\infty}(1/2)A^{r-2}BP_{1,0}^2 r^2} = \frac{A^{r-2}r^2}{\sum_{r=2}^{\infty}A^{r-2}r^2} \tag{C.2}$$

Making the long-chain assumption, Eq. (C.2) reduces to:

$$f(r,1) = \frac{1}{2}A^{r-4}r^2(1-A)^3 \tag{C.3}$$

Since $A \rightarrow 1$ for long chains, Eq. (C.3) can be also expressed as:

$$f(r,1) = \frac{1}{2}r^2(1-A)^3\exp[-r(1-A)] = \frac{1}{2}r^2\tau^3\exp(-r\tau) \tag{C.4}$$

Chain length averages predicted with Eq. (C.4) agree with the ones calculated by the method of the moments:

$$\bar{r}_{n,1} = \int_0^{\infty} f(r,1)\mathrm{d}r = \frac{3}{\tau} = 3\bar{r}_{n,0} \tag{C.5}$$

$$\bar{r}_{w,1} = \left(\int_0^{\infty} r^2 f(r,1)\mathrm{d}r\right)\left(\int_0^{\infty} rf(r,1)\mathrm{d}r\right)^{-1} = \frac{4}{\tau} = 2\bar{r}_{w,0} \tag{C.6}$$

Repeating the same steps for populations with 2, 3, ..., n LCB/chain one obtains the general expressions given by Eqs. (46) and (47). All derivation steps were verified with MAPLE V [18].

Average values for long chain branching frequency can be also easily obtained by noticing that:

$$\bar{B}_N = \left(\frac{R_{LCB}}{R_{cf}}\right) = \frac{k_{pLCB}Q_0^{=}}{k_\beta + k_{CTA}[CTA] - k_{pLCB}Q_0^{=}} \tag{C.7}$$

where

$\bar{B}_N$ average number of LCB per polymer chain
R_{cf} net rate of dead polymer chain formation
R_{LCB} rate of macromonomer propagation

Observe that $\bar{B}_N$ calculated using Eq. (C.7) agrees with the values obtained from the whole distribution as shown in Tab. 3.

It is also easy to calculate the number of LCB per 1000 carbon atoms, $\bar{\lambda}_N$:

$$\bar{\lambda}_N = 500\frac{R_{LCB}}{R_p} = \frac{k_{pLCB}Q_0^{=}}{k_pM} \tag{C.8}$$

Appendix D: Equations for copolymerization using pseudo-kinetic rate constants

The equations derived for homopolymerization can be used for copolymerization by simply replacing the kinetic rate constant with pseudo-kinetic rate constants as described by Hamielec et al. [9]

The parameter τ in Eq. (47) can be defined for a homo- or copolymerization simply as:

$$\tau = \frac{R_\beta}{R_p} + \frac{R_{CTA}}{R_p} + \frac{R_{LCB}}{R_p} \tag{D.1}$$

where

R_β rate of β-hydride elimination
R_p rate of monomer propagation
R_{CTA} rate of transfer to chain transfer agent
R_{LCB} rate of macromonomer propagation

assuming that the chains are long and therefore $R_p \gg R_\beta + R_{CTA} + R_{LCB}$.

R_p, R_β, R_{CTA} and R_{LCB} can be calculated for a binary copolymerization using the terminal model as follows:

$$\begin{aligned} R_p = {} & k_{p11}(\text{Cat} - \text{M}_1)M_1 + k_{p12}(\text{Cat} - \text{M}_1)M_2 \\ & k_{p21}(\text{Cat} - \text{M}_2)M_1 + k_{p22}(\text{Cat} - \text{M}_2)M_2 \end{aligned} \tag{D.2}$$

$$R_\beta = k_{\beta 1}(\text{Cat} - \text{M}_1)M_1 + k_{\beta 2}(\text{Cat} - \text{M}_2) \tag{D.3}$$

$$R_{CTA} = k_{CTA1}(\text{Cat} - \text{M}_1)[\text{CTA}] + k_{CTA2}(\text{Cat} - \text{M}_2)[\text{CTA}] \tag{D.4}$$

$$R_{LCB} = k_{pLCB1}(\text{Cat} - \text{M}_1)Q_0^{=} + k_{pLCB2}(\text{Cat} - \text{M}_2)Q_0^{=} \tag{D.5}$$

where $\text{Cat} - \text{M}_i$ represents a living polymer chain terminated by monomer of type i, and the subscripts 1 and 2 in the kinetic rate constants indicate rates for monomer types 1 and 2 and for living polymer chains terminating with monomers type 1 and 2, as usually defined for the terminal model for copolymerization.

Nomenclature

A defined in Eq. (12)
B defined in Eq. (13)
$\bar{B}_N$ average number of LCB per polymer chain, Eq. (C.7)
[CTA] concentration of chain transfer agent, in mol/L
$D_{r,i}^{=}$ concentration of dead polymer of chain length r containing i long chain branches and with terminal vinyl unsaturation (macromonomer), in mol/L
$D_{r,i}$ concentration of dead polymer of chain length r containing i long chain branches and with saturated chain end, in mol/L
$f(r,n)$ frequency distribution of chain length for population with n LCB/chain, Eqs. (46) and (47)
k_{CTA} rate constant for transfer to chain transfer agent, in L/(mol · s)
k_p propagation rate constant for monomer, in L/(mol · s)
k_{pLCB} propagation rate constant for macromonomer, L/(mol · s)
k_β rate constant for β-hydride elimination, in 1/s
K_T defined in Eq. (7)
M monomer concentration, in mol/L

pdi_i	polydispersity index for population with i LCB/chain; if i not shown, indicates average value over all populations
P_{pT}	probability of propagation
P_p	probability of monomer propagation
P_{pLCB}	probability of macromonomer propagation
$P_{r,i}$	concentration of living polymer of chain length r containing i long chain branches, in mol/L
P_t	probability of chain transfer/termination
$Q_j^=$	j^{th} moment of dead polymer chains with terminal vinyl unsaturation for all populations, in mol/L
$\bar{r}_{n,i}$	number-average chain length for population with i LCB/chain; if i not shown, indicates average value over all populations
$\bar{r}_{w,i}$	weight-average chain length for population with i LCB/chain; if i not shown, indicates average value over all populations
$\bar{r}_{z,i}$	z-average chain length for population with i LCB/chain; if i not shown, indicates average value over all populations
R_β	rate of β-hydride elimination, in mol/(L·s)
R_p	rate of monomer propagation, in mol/(L·s)
R_{CTA}	rate of transfer to chain transfer agent, in mol/(L·s)
R_{LCB}	rate of macromonomer propagation, in mol/(L·s)
s	reciprocal of the mean residence time in reactor, in 1/s
Y_j	j^{th} moment of living polymer for all populations, in mol/L
$Y_{j,i}$	j^{th} moment of living polymer for population with i LCB/chain, in mol/L
t	time, in s
α	defined in Eq. (A.12)
γ	defined in Eq. (14)
τ	defined as $1 - A$, see also Eq. (D.1)

[1] U.S. Patent 5,272,236 (1993), invs.: S. Y. Lai, J. R. Wilson, G. W. Knight, J. C. Stevens, P. W. S. Chum, *"Elastic substantially linear olefin polymers"*

[2] U.S. Patent Application WO 93/08221 (1993), invs.: S. Y. Lai, J. R. Wilson, G. W. Knight, J. C. Stevens, *"Elastic substantially linear olefin polymers"*

[3] K. W. Swogger, C. I. Kao, in *"Polyolefins VIII", Tech. Pap., Reg. Tech. Conf. – Soc. Past. Eng.* 14 (1993)

[4] J. C. Randall, *"Polymer Sequence Distribution, Carbon-13 NMR Method"*, Academic Press, New York 1977

[5] J. B. P. Soares, A. E. Hamielec, *Polymer* **36**, 2257 (1995)

[6] P. J. Flory, *"Principles of Polymer Chemistry"*, Ithaca, Cornell University Press 1953

[7] J. Huang, G. L. Rempel, *Prog. Polym. Sci.* **20**, 459 (1995)

[8] M. Sugawara, Proceedings of the 4th International Business Forum on Specialty Polyolefins, Houston, Texas, USA, 37 (1994)

[9] A. E. Hamielec, J. F. MacGregor, A. Penlidis, *Makromol. Chem., Macromol. Symp.* **10/11**, 521 (1987)

[10] L. Resconi, F. Piemontesi, G. Franciscono, L. Abis, T. Fiorani, *J. Am. Chem. Soc.* **114**, 1025 (1992)

[11] Dow European Patent Application 0416815A2, August 30 (1990)
[12] International Patent Application WO-94/07930, April 14, Exxon Chemical Patent Inc. (1994), invs.: P. Brant, J. A. M. Kanich, D. A. Jay, R. L. Bamberger, G. F. Licciardi, P. M. Henrichs
[13] J. M. Vela-Estrada, A. E. Hamielec, *Polymer* **19**, 808 (1994)
[14] J. B. P. Soares, A. E. Hamielec, *Polym. React. Eng.* **3**, 131 (1995)
[15] F. Garbassi, L. Gila, A. Proto, *Polym. News* **19**, 367 (1994)
[16] J. B. P. Soares, A. E. Hamielec, *Polym. React. Eng.* **3**, 261 (1995)
[17] W. H. Stockmayer, *J. Chem. Phys.* **13**, 199 (1945)
[18] M. L. Abell, J. P. Braselton, *"MAPLE V by Example"*, Academic Press Cambridge, MA 1994
[19] G. W. Knight, S. Lai, in *"Polyolefins VIII", Tech. Pap., Reg. Tech. Conf. — Soc. Plast. Eng.* 28 (1993)